

Including Atmospheric Extinction in a Performance Evaluation of a Fixed Grid of Solar Panels

Kevin Krisciunas^{1,2}

ABSTRACT

Solar power is being used to satisfy a higher and higher percentage of our energy needs. We must be able to evaluate the performance of the hardware. Here we present an analysis of the performance of a fixed grid of 13 solar panels installed in the spring of 2021. We confirm that the power output is linearly proportional to the cosine of the angle of the incidence of sunlight with respect to the vector perpendicular to the panels. However, in order to confirm this, we need to consider the dimming effect of the Earth's atmosphere on the intensity of the Sun's light, which is to say we need to rely on astronomical photometric methods. We find a weighted mean value of 0.168 ± 0.007 mag/airmass for the extinction term, which corresponds to the sea level value at a wavelength of about 0.76 microns. As the efficiency of the solar panels is expected to degrade slowly over time, the data presented here provide a baseline for comparison to the future performance of the system.

Subject headings: photometry - techniques

1. Introduction

On 26 April 2021 Texas Green Energy installed two sets of solar panels³ on my house in College Station, Texas (latitude $+30.56^\circ$, longitude W 96.27° , elevation 103 m). Six panels are mounted on the upper roof, and seven panels on the lower roof. After engineers, technicians, and city inspectors were done with their work, the system went live on 8 June.

¹Texas A. & M. University, Department of Physics & Astronomy, 4242 TAMU, College Station, TX 77843; krisciunas@physics.tamu.edu

²George P. and Cynthia Woods Mitchell Institute for Fundamental Physics & Astronomy

³Engineered in Germany by Q.CELLS, the panel model is Q.PEAK DUO BLK-G6+ 330-345. Basic information on photovoltaic cells can be found here: <https://www.energy.gov/eere/solar/articles/pv-cells-101-primer-solar-photovoltaic-cell>

According to the installers, the panels face azimuth 135° (i.e. due southeast). The pitch of each roof is 24° . The vector perpendicular to the panels intersects the celestial sphere at azimuth 135° and elevation angle 66° in the horizon system of celestial coordinates.⁴ Let us call this position P. Its elevation angle and azimuth must have some uncertainty (± 1 or 2 degrees in each coordinate). Such uncertainty will not have a *significant* effect on the main results presented here, as some experiments assuming azimuth 128° , elevation angle 70° for point P showed.

For an object like the Sun that transits the celestial meridian south of the zenith for an observer in the northern hemisphere situated north of the Tropic of Cancer,⁵ the maximum elevation angle above the horizon will be:

$$h_{max} = [90^\circ - \phi] + \delta_\odot, \quad (1)$$

where ϕ is the latitude of the observer and δ_\odot is the declination of the Sun. Given my latitude of about 30.6° and the declination of the Sun in June (roughly $+23^\circ$), for my site the maximum elevation angle of the Sun is between 82° and 83° .

Let θ be the angular distance between position P mentioned above and the direction towards the Sun. Of course, due to the rotation of the Earth, the elevation angle and azimuth of the Sun change continuously, so θ changes continuously.

Fig. 1 is a plot of raw data obtained from 9 to 26 June 2021 and tabulated in Table 1. The reader will notice that the dataset is not symmetric. The reason is that starting about 15:15 CDT each day in June part of the house casts a larger and larger shadow on some of the lower panels. We will not consider any further those measurements in Table 1 taken after 15:15 local time.

According to the specifications on solar panels, their output varies proportional to $\cos(\theta)$. This can be demonstrated in the lab, or outside using the Sun as the illumination source. Here we shall demonstrate this cosine law. But first we must discuss some basics of astronomical photometry.

⁴Basic information on the celestial sphere can be found online at http://people.tamu.edu/~kevinkrisciunas/cel_sphere.html.

⁵In Hilo, Hawaii, for example, at latitude $+19.7^\circ$, the Sun transits the celestial meridian *north* of the zenith for about two months each year starting on May 18th.

2. Astronomical Photometry

Astronomical photometry dates back to the time of Hipparchus (ca. 150 B.C.), who classified the brightness of the stars using magnitude bins. The brightest stars in the sky were defined to be magnitude 1 (i.e. stars of the first class), while the faintest stars visible to the unaided eye were magnitude five or six. Using a nineteenth century formulation of magnitudes, a first magnitude star gives us exactly 100 times as many photons per second as a sixth magnitude star. In the nineteenth century Karl August Steinheil and Gustav Theodor Fechner demonstrated that the impression we have of the brightness of a light source is proportional to the logarithm of the light intensity. This relationship holds for hearing and for taste and is known as the Weber-Fechner psychophysical law (Herrmann 1984, pp. 70-76).

If we measure a signal of f_1 photons per second from one star and f_2 from a second (fainter) star, then $2.5 \log_{10} (f_1/f_2) = \Delta m$, the *difference* of their magnitudes, with the fainter star having the larger arithmetic value. Similarly, $a^{\Delta m} = f_1/f_2$, where a is equal to the fifth root of 100, or approximately 2.51186.

Consider a schematic diagram of a plane parallel atmosphere (Fig. 2). A star at zenith angle z is observed through a longer path length of atmosphere than it would be at the zenith. For $z < 60^\circ$ that path length, divided by the path length towards the zenith, is simply $\sec(z)$. We call the ratio of these path lengths the “air mass” (X), which is a unitless parameter. It is *not* a column density of molecules and atoms measured through the atmosphere. For $z < 60^\circ$, $X = \sec(z)$ is calculated geometrically.

For zenith angles greater than 60° (i.e., air mass greater than 2.0) the plane parallel approximation of the atmosphere breaks down. After all, the atmosphere is a spherical shell. Also, for objects viewed near the horizon we have to consider atmospheric refraction. These considerations are beyond the scope of the present paper. For our purposes here we may use the following formula from Hardie (1962):

$$X = \sec z - 0.0018167 (\sec z - 1) - 0.002875 (\sec z - 1)^2 - 0.0008083 (\sec z - 1)^3 . \quad (2)$$

Nowadays we take celestial images using a telescope and solid state cryogenically-cooled charge-coupled device (CCD), using a number of photometric filters, such as a blue filter called B and a yellow-green filter called V . These two filters have transmission curves that peak at about 440 and 550 nm, respectively. Instrumental magnitudes can be determined by displaying the images with SAO Image DS9 and doing aperture photometry in the IRAF

environment.⁶

How does one reduce the data? Experts give conflicting advice. As my colleague George Wallerstein (1930-2021) used to say, “Four astronomers, five opinions.” For simplicity’s sake, using software like IRAF one designates the radius in pixels of an aperture, centers one star in the aperture, and determine the number of digital counts above the sky level. IRAF calculates *minus* $2.5 \log_{10}$ of those counts and adds $2.5 \log_{10}$ of the integration time in seconds.⁷ This gives an instrumental magnitude adjusted to an integration time of one second. From the telescope operating system the image files contain the air mass values.

Say one has taken B -band and V -band images of fields of standard stars, such as those of Landolt (1992, 2007). One ends up with instrumental b and v magnitudes. The simplest transformation of the instrumental v magnitudes and instrumental $b - v$ colors to standardized V -band values in the photometric system of Landolt is:

$$V = v - k_v X + CT_v(b - v) + \zeta_v, \quad (3)$$

where: k_v is the V -band atmospheric extinction coefficient; CT_v is a color term used to correct for differences of transmission as a function of wavelength of the filters used by you and the ones used by Landolt; and ζ_v is a photometric zero point (or, simply, the Y-intercept of some regression line). If the stars range in color from very blue to very red and/or the observations were made over a wide range of air mass, one may have to add second order terms to Eq. 3.

Using IRAF or equivalent FORTRAN or PYTHON code, one can solve simultaneously for the extinction term, color term, and zero point. (We are effectively fitting the best plane to a three dimensional set of data.) If the color term is known, then one can take the difference of the color-corrected instrumental v magnitudes and Landolt’s standardized values and plot these magnitude differences vs. the air mass values to obtain the extinction term and the photometric zero point.

Fig. 3 shows an example of determining the atmospheric V -band extinction coefficient, using data taken by us with the 0.9-m telescope at Cerro Tololo Inter-American Observatory (CTIO) on 26 November 2005 (UT). The magnitude differences get fainter (i.e. become

⁶IRAF is distributed by the National Optical Astronomy Observatory, which is operated by the Association of Universities for Research in Astronomy, Inc., under cooperative agreement with the National Science Foundation (NSF).

⁷IRAF also adds an arbitrary constant here, defaulted to 25. This is to give instrumental magnitudes that are positive and comparable to what the eventual reduced values become.

more positive) as we observe stars lower in the sky (i.e. at higher air mass). If the sky is clear and has stable transparency, one can convert all of the raw measurements taken on a given night to standardized, publishable values, with random errors of ± 0.02 magnitudes or better (roughly 2 percent). In Fig. 3 we find a V -band extinction coefficient of 0.164 ± 0.005 mag/airmass and a root-mean-square (RMS) residual of ± 0.013 mag, after eliminating one $5\text{-}\sigma$ outlier from the regression. This may be compared to the median V -band extinction of 0.154 mag/airmass from 29 nights of observations by us at CTIO and Las Campanas Observatory (LCO) from 21 April 2001 through 21 December 2012. In our experience, under clear sky conditions the extinction values in a particular photometric band at a particular site vary from night to night at least ± 50 percent compared to the mean or median value.

3. Demonstrating the Cosine Law

One records the power output by the solar panel system (from a digital display) over a wide range of the Sun’s elevation angle on a clear day. One then proceeds to calculate the elevation angle and azimuth of the Sun for each observation time using the right ascension and declination of the Sun. One can look up α_{\odot} and δ_{\odot} in the annual volume of the *Astronomical Almanac* and interpolate to local noontime for any given day. Or one can use the method of van Flandern & Pulkkinen (1979) to obtain α_{\odot} and δ_{\odot} to the nearest arc minute.⁸

Using a program written by us, one can set the date, latitude and longitude of the site, and the right ascension and declination of the Sun to calculate the Sun’s azimuth, elevation angle, and air mass for all the corresponding times of day. Then, one calculates the values of angle θ , the angular distance between point P (azimuth 135° , elevation angle 66°) and the azimuth and elevation angle of the Sun at the times in question. A plot of the measured power (P_{meas}) vs. $\cos(\theta)$ from 16 June 2021 is found in the top half of Fig. 4. It is encouraging that the data show a linear relation, but it is clear that a linear fit to the data does not pass through the origin. It certainly should do so, because the panels begin generating power in the early morning once the Sun’s light is incident on the panels.

We can correct the measured values of the power to the equivalent values we would have obtained if the Sun were at the zenith, as follows:

$$P_{extcorr} = 2.51186^{k_{\lambda}(X_{\odot} - 1)} \times P_{meas} , \quad (4)$$

⁸A table of the Sun’s coordinates for each day of this year can be found here: http://people.tamu.edu/~kevinkrisciunas/ra_dec_sun_2021.html

where k_λ is an effective extinction term corresponding to the response of the solar panels over whatever wavelength range they are sensitive, and X_\odot is the air mass of the Sun.

Consider making a plot like the top half of Fig. 4, but scale the measured values of the power by the scaling factor in Eq. 4, with $k_\lambda = 0.10$. Fit a line to the data and keep track of the Y-intercept of the plot (and its uncertainty). Do this again for extinction 0.12, 0.14, 0.16, and 0.18, for example. Then plot those Y-intercepts vs. the trial extinction values and derive what extinction value would give a Y-intercept of 0.0. In the bottom part of Fig. 4 we see that an extinction term of 0.140 mag/airmass works best for 16 June 2021.

We note that the first point of the day on 16 June was taken when the Sun’s elevation angle was 3.03° (zenith angle 86.97°) and its airmass (from Eq. 2) was 13.311. With an extinction term of 0.140 mag/airmass, the measured power of 137 Watts implies that the solar panels would have produced 670 Watts (4.89 times as much) if the Sun had been at the zenith and the solar panels had been tilted to keep angle θ the same (79.39°).

In Table 2 we give the derived values of the extinction term for 13, 14, 16, 19, 23, and 26 June 2021. The values range from 0.140 to 0.212 mag/airmass. The weighted mean value is 0.168 ± 0.007 mag/airmass. For 10, 15, 17, and 18 June we did not have sufficient measurements over a wide range of airmass to derive the extinction term. For those dates we adopt the weighted mean value from the other days.

For comparison we can consider values of the V -band extinction measured essentially at sea level. At the nearby Texas A&M Physics Observatory during the colder months the V -band extinction values range between 0.2 and 0.3 mag/airmass (Carona 2021, private communication). From nine nights of observations near Los Gatos, California (elevation 80 m), from October 1981 to March 1982 we measured mean V -band extinction of $k_v = 0.341 \pm 0.050$ mag/airmass. At 75 m elevation near Keaau, Hawaii, on 19 December 1989 (UT) we measured $k_v = 0.341 \pm 0.020$ mag/airmass on a night that was affected by some volcanic haze. On the next night (clear, but with strong scintillation) we measured $k_v = 0.187 \pm 0.046$ mag/airmass (Krisciunas 1990).

Let us also consider the range of optical extinction from the near ultraviolet to the end of the optical range of wavelengths as measured by us on 29 nights at CTIO (elevation 2200 m) and LCO (2380 m); see Fig. 5. Extinctions measured at a mountaintop observatory are of course lower than one would measure at sea level because there is less atmosphere above a mountain to dim the light of celestial objects.⁹

⁹We also note that Table 4 of Krisciunas et al. (2017) gives mean extinctions derived from observations of 2004 to 2009 with the 1-m Swope telescope at Las Campanas as part of the Carnegie Supernova Project.

We can determine the effective range of wavelengths for which the solar panels are functional.¹⁰ It all has to do with the physics of the photovoltaic effect, which takes place at the boundary of two semiconducting plates. One key parameter is the “band gap energy” of silicon. Only photons with energy greater 1.11 electron volts can dislodge electrons from silicon atoms and send them into the conduction band between the two semiconducting plates. The longest wavelength light usable by the solar panels is near-infrared light at 1.1 microns. Photons with energy greater than 3 eV send electrons out of the conduction band, rendering them unable to do work. The corresponding wavelength is about 413 nanometers (i.e violet light). Thus, solar panels convert sunlight with wavelengths ranging from 0.413 to 1.1 microns into electric power. This author does not know of a “response curve” of solar panels as a function of wavelength, but the mean wavelength of sensitivity is about 760 nm. This is between the effective wavelengths of the photometric *R*- and *I*-bands at 650 and 800 nm, respectively (or the corresponding Sloan *r*- and *i*-bands).

On the basis of the median extinction values at CTIO and LCO we can estimate that the extinction at 0.76 microns is about 50 percent of the value of the *V*-band extinction. If the *V*-band extinction at sea level ranges from 0.24 to 0.36 mag/airmass, the 0.76 micron extinction should be roughly 0.12 to 0.18 mag/airmass. This range is comparable to the values given in Table 2 that apply to the solar panels. Thus, in the analysis of the performance of the solar panels we feel confident that by trying a range of values of extinction in Eq. 4 to get a regression through the origin, as in the lower half of Fig. 4, on a given day we are actually deriving a sensible value of the atmospheric extinction of light corresponding to the long wavelength end of the optical spectrum.

In Fig. 6 we combine all the solar panel data taken prior to 15:15 CDT on all the days and confirm the cosine law:

$$P_{extcorr} = 3819 \cos(\theta) \text{ (Watts)} . \quad (5)$$

The RMS residual of the regression through the origin in Fig. 6 is ± 143 W. We note, however, that for $\cos(\theta)$ less than 0.75 (θ greater than 41.4°) the RMS residual is ± 98 W, while for $\cos(\theta)$ greater than 0.75 the RMS residual is ± 184 W. There is more scatter in the data when the Sun is high in the sky, as one can surmise from the raw data shown in Fig. 1. The *relative* scatter appears approximately constant as a function of $\cos(\theta)$.

We found mean extinction values of $k_u = 0.511$, $k_B = 0.242$, $k_V = 0.144$, $k_r = 0.103$, and $k_i = 0.059$ mag/airmass.

¹⁰See: <https://sciencing.com/effect-wavelength-photovoltaic-cells-6957.html>

The technical specifications from the manufacturer of the solar panels indicate that the relative efficiency of the panels will degrade from 98 to roughly 83 percent over their 25 year lifetime. The data presented here can be used as a baseline to evaluate the future performance of the solar panels.¹¹

We thank Don Carona and Nick Suntzeff for useful discussions.

¹¹Another test that can be done in the near term is to hope for clear skies on or about 19 August 2021 and 22 April 2022, when the Sun will pass through the vector perpendicular to the panels ($\theta = 0.0$) at my site.

REFERENCES

- Hardie, R. H. 1962, in Stars and Stellar Systems, 2, Astronomical Techniques, ed. W. A. Hiltner (Chicago: Univ. of Chicago Press), 178.
- Herrmann, D. B. 1984, The History of Astronomy from Herschel to Hertzsprung, transl. K. Krisciunas (Cambridge: Cambridge Univ. Press)
- Krisciunas, K. 1990, PASP, 102, 1052
- Krisciunas, K., Contreras, C., Burns, C. R., et al. 2017, AJ, 154, 211
- Landolt, A. U. 1992, AJ, 104, 372
- Landolt, A. U. 2007, AJ, 133, 2502
- Van Flandern, T. C. & Pulkkinen, K. F. 1979, ApJS, 41, 391

Table 1. Raw Data^a

Date	CDT	P_{meas}	AZ_{\odot}	EL_{\odot}	X_{\odot}	θ
9 June	16:07	1779	268.19	53.13	1.2499	55.68
	17:10	863	275.76	39.55	1.5703	70.20
10 June	12:31	3859	118.62	75.78	1.0316	11.06
	13:38	3545	201.83	81.95	1.0099	22.04
	14:51	3266	253.24	69.82	1.0654	37.71
	16:16	1322	269.47	51.26	1.2820	57.01
	17:10	680	275.83	39.63	1.5679	70.13
13 June	8:19	1579	75.36	22.35	2.6153	57.48
	9:20	2459	81.73	35.25	1.7327	43.46
	10:06	2885	86.77	45.12	1.4112	33.02
	10:55	3278	93.01	55.70	1.2106	22.33
	11:48	3744	102.65	67.03	1.0862	12.79
	12:24	3909	114.29	74.41	1.0382	10.83
	13:30	3905	187.75	82.61	1.0084	20.34
14 June	7:23	513	69.22	10.82	5.2009	70.40
	7:44	900	71.55	15.09	3.7950	65.58
	8:04	1240	73.70	19.21	3.0172	60.99
	8:24	1539	75.81	23.37	2.5086	56.38
	8:41	1812	77.59	26.94	2.1993	52.47
	9:05	2131	80.08	32.02	1.8858	46.96
	9:48	2595	84.66	41.22	1.5176	37.13
	10:10	2801	87.14	45.96	1.3912	32.18
	11:03	3187	94.07	57.39	1.1872	20.75
	15 June	16:46	822	273.37	45.11	1.4114
17:18		586	276.91	38.23	1.6158	71.71
17:53		363	280.59	30.77	1.9547	79.69
16 June	6:45	137	64.53	3.03	13.311	79.39
	7:06	402	67.04	7.17	7.7826	74.61
	7:32	840	70.01	12.39	4.5764	68.66
	7:52	1181	72.20	16.47	3.4907	64.07
	8:03	1375	73.38	18.74	3.0883	61.54
	8:31	1823	76.32	24.57	2.3943	55.10
	9:08	2225	80.16	32.39	1.8668	46.60
	10:03	2923	86.08	44.17	1.4352	34.08
	10:30	3152	89.27	49.99	1.3056	28.08
	11:18	3412	96.10	60.33	1.1508	18.11
	11:54	3531	103.43	67.59	1.0786	12.40
	12:28	3584	114.98	74.94	1.0356	11.05
	13:03	3827	141.54	80.98	1.0125	15.07
	17 June	8:17	1580	74.91	21.82	2.6753
9:13		2330	80.74	33.63	1.8057	45.27
12:24		3554	113.44	74.31	1.0387	10.95
14:03		3569	130.77	79.15	1.0182	27.19
18 June	12:00	3641	105.04	69.39	1.0684	11.73
	12:58	3711	136.40	80.39	1.0142	14.39
	13:56	3747	224.12	80.32	1.0145	25.63

Table 1—Continued

Date	CDT	P_{meas}	AZ_{\odot}	EL_{\odot}	X_{\odot}	θ
	15:11	3060	259.23	65.71	1.0972	42.39
	15:32	2312	263.29	61.23	1.1409	47.20
19 June	7:23	697	68.98	10.67	5.2698	70.63
	7:59	1297	72.93	18.01	3.2067	62.38
	9:06	2264	79.93	32.06	1.8839	46.98
	10:27	3074	88.85	49.44	1.3163	28.69
	11:17	3371	95.88	60.22	1.1522	18.26
	11:46	3518	101.46	66.40	1.0912	13.38
	13:08	3873	148.20	81.70	1.0106	16.03
	14:12	3426	237.29	77.68	1.0236	29.07
	15:15	2720	260.06	64.91	1.1042	43.26
	15:46	1993	265.57	58.27	1.1757	50.37
	16:45	900	273.28	45.55	1.4009	63.93
	17:14	674	276.50	39.31	1.5785	70.58
	17:35	501	278.72	34.82	1.7514	75.38
23 June	7:03	324	66.59	6.49	8.2685	75.41
	7:29	744	69.57	11.69	4.8333	69.47
	7:59	1266	72.85	17.82	3.2389	62.58
	8:32	1773	76.33	24.69	2.3838	54.99
	9:06	2237	79.85	31.87	1.8941	47.18
26 June	7:03	299	66.59	6.32	8.4534	75.56
	7:25	665	69.13	10.72	5.2457	70.53
	8:23	1684	75.41	22.64	2.5843	57.20
	8:46	2050	77.80	27.47	2.1606	51.91
	9:19	2554	81.24	34.47	1.7668	44.33
	9:44	2944	83.90	39.82	1.5615	38.63

^aColumn by column we give the 2021 date, the Central Daylight Time in hours and minutes, the measured power (in W) from the solar panels, the Sun’s azimuth and elevation angle in degrees, the Sun’s air mass, and the angle in degrees between the vector perpendicular to the solar panels and the direction toward the Sun.

Table 2. Derived Extinction Values^a

Date	Extinction (mag/airmass)	N
13 June	0.212 ± 0.058	7
14 June	0.194 ± 0.048	9
16 June	0.140 ± 0.024	13
19 June	0.148 ± 0.056	9
23 June	0.161 ± 0.014	5
26 June	0.182 ± 0.014	6
Weighted mean	0.168 ± 0.007	

^aYear = 2021. N is the number of points.

Fig. 1.— Measured power (in Watts) from the solar panels as a function of time of day. Color coding: 13 June (magenta); 14 June (blue); 16 June (cyan); 19 June (green); 23 June (orange); 26 June (red); 9, 10, 15, 17, and 18 June (grey). The vertical dashed line indicates the time of day in June 2021 when the house begins casting a shadow on some of the panels in the lower set of seven.

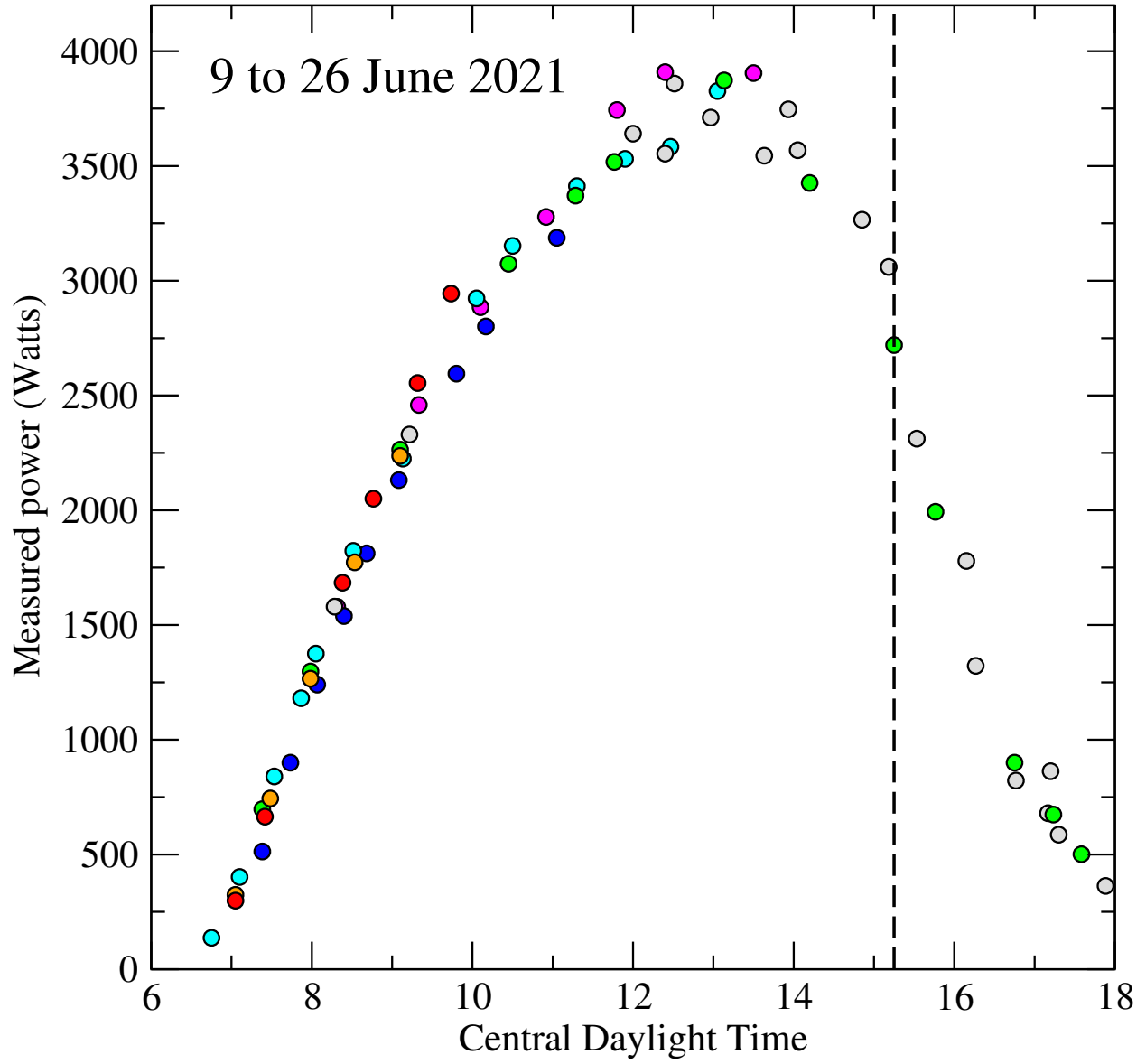
Fig. 2.— The plane parallel atmosphere model. Ground level is represented by the solid horizontal line. The extent of the atmosphere is represented by the dashed line. A star at zenith angle z is observed through a path length of atmosphere that is approximately equal to $\sec(z)$ times the path length in the direction of the zenith. This ratio of path lengths is called the “air mass” (X).

Fig. 3.— The difference of the color-corrected instrumental V -band magnitudes of photometric standards *minus* the standardized V -band magnitudes from Landolt (1992, 2007) versus the air mass value (secant of the zenith angle). The data were taken with the 0.9-m telescope at Cerro Tololo Inter-American Observatory by the author on 26 November 2005 (UT). The yellow triangle represents a very blue star measured at high air mass. As it is a $5\text{-}\sigma$ outlier, it has been eliminated from the fit.

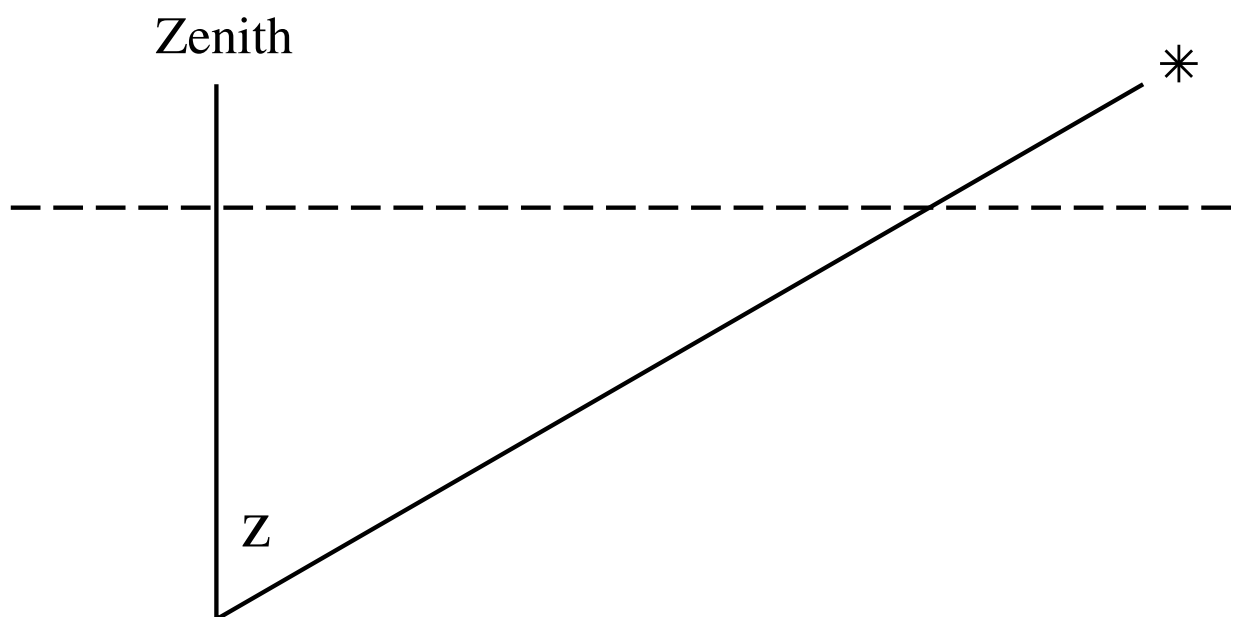
Fig. 4.— *Top*: The measured power output of the solar panel system (in Watts) on 16 June 2021 as a function of the cosine of the angular distance between the vector perpendicular to the solar panels and the direction toward the Sun. The regression line clearly does not pass through the origin. *Bottom*: Same as top diagram, except the power has been corrected to what would have been measured if the Sun were at the zenith and the panels were tilted to the same values of angle θ .

Fig. 5.— The median atmospheric extinction at Cerro Tololo and Las Campanas as a function of wavelength, based on 29 nights of observations by us from 21 April 2001 to 21 December 2012. The filters used were Johnson U , B , and V , Cousins R and I , and Sloan u , r , and i . The dashed line corresponds to the mean wavelength of functionality of solar panels with silicon-based photovoltaic cells.

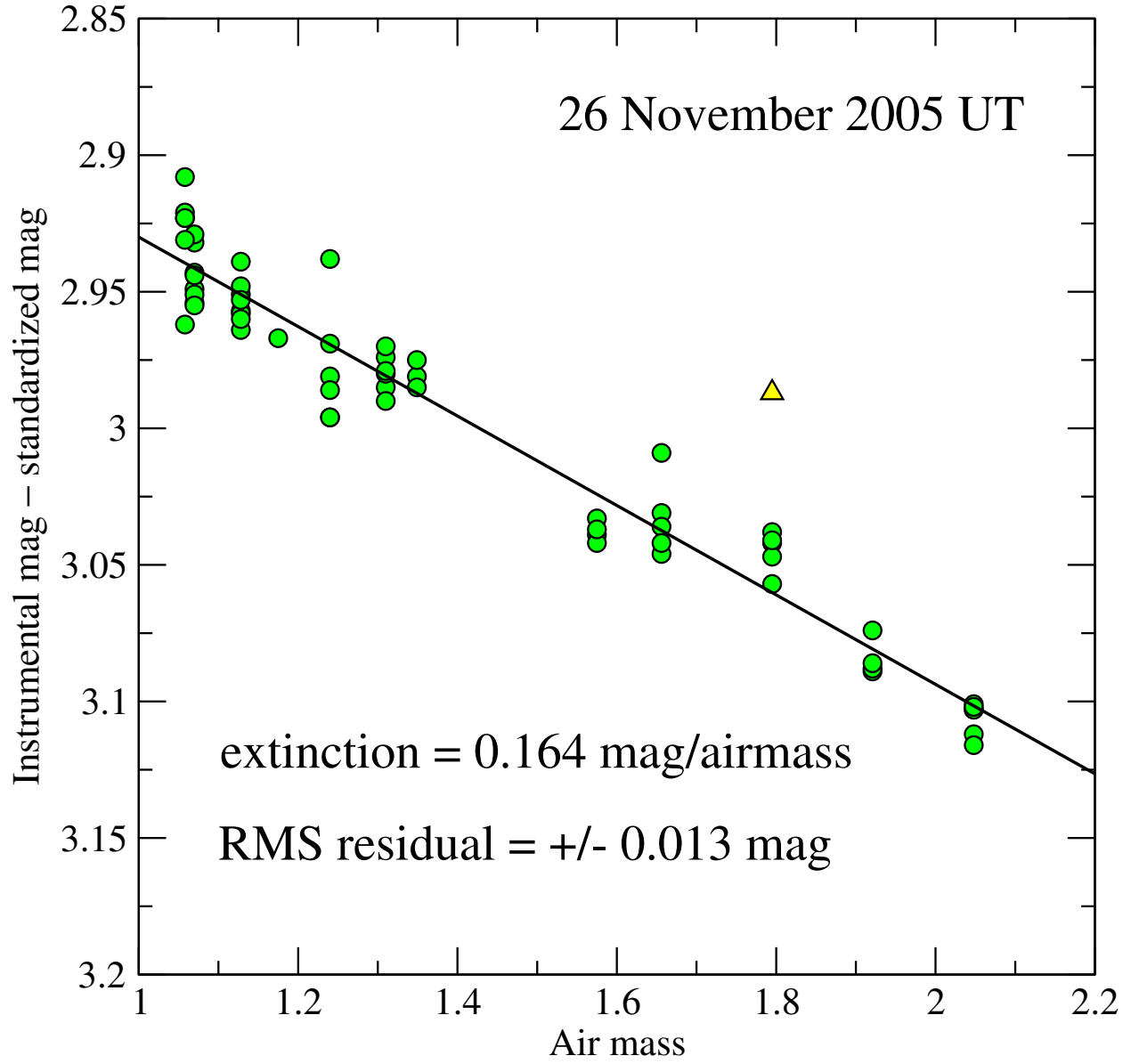
Fig. 6.— Demonstration of the cosine law response of the array of solar panels. The measured values of the power from the solar panels have been corrected for the amount of atmospheric extinction affecting the Sun’s intensity, with respect to the Sun being at the zenith. The color coding of the points is the same as in Fig. 1.



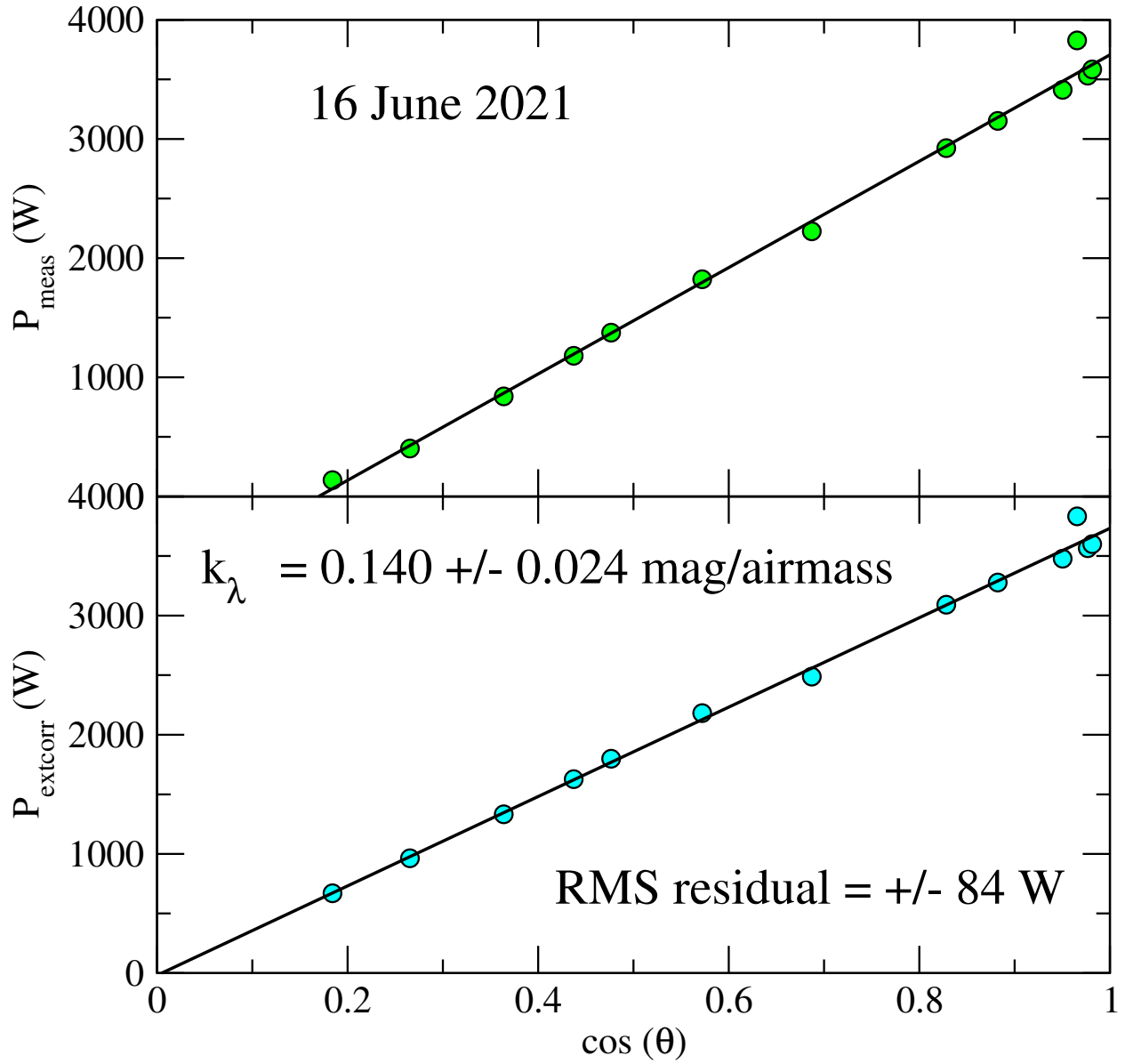
Krisciunas Fig. 1.



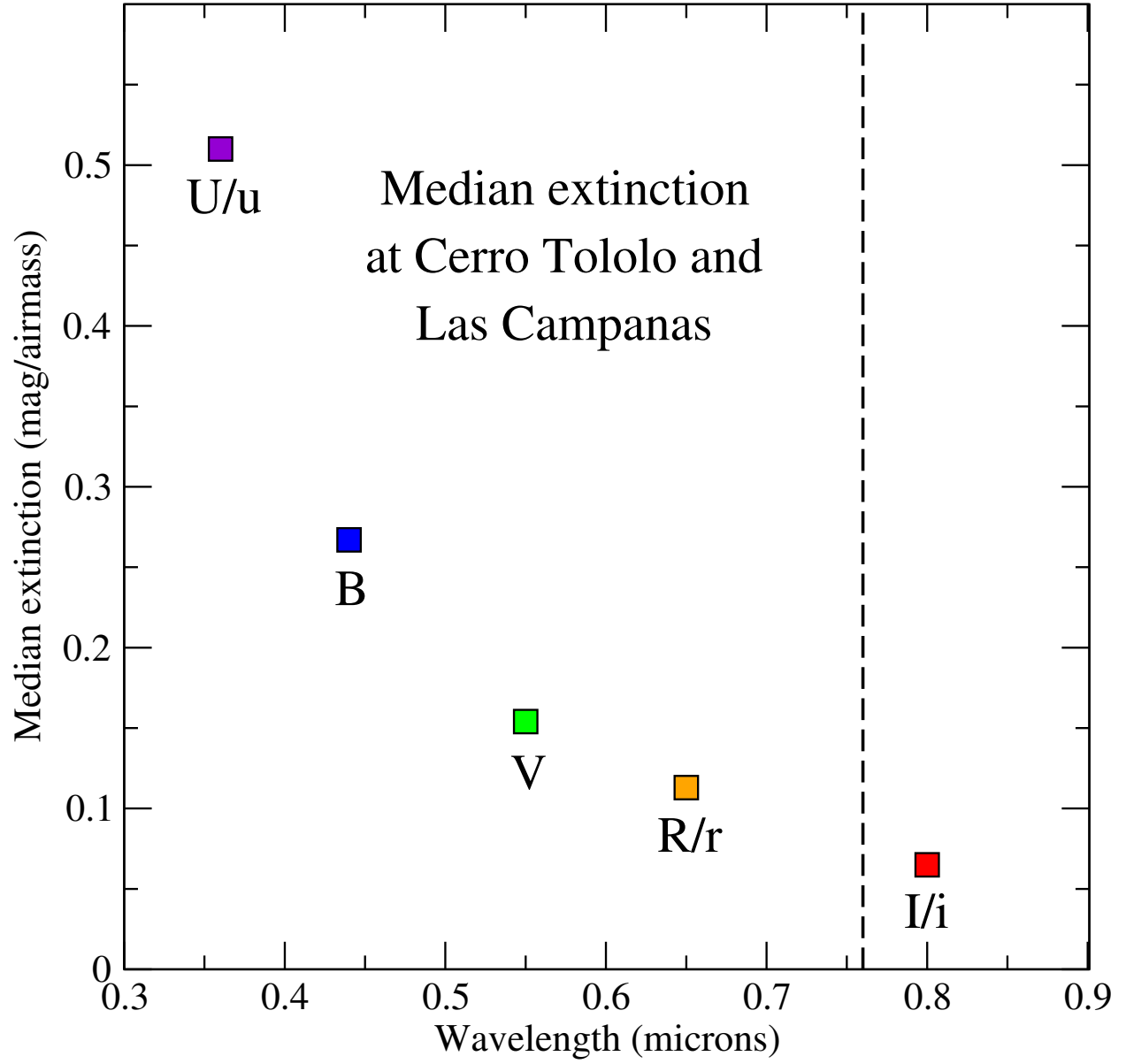
Krisciunas Fig. 2.



Krisciunas Fig. 3.



Krisciunas Fig. 4.



Krisciunas Fig. 5.

